Cleaner and Responsible Consumption 3 (2021) 100040

Contents lists available at ScienceDirect

Cleaner and Responsible Consumption

journal homepage: www.journals.elsevier.com/cleaner-and-responsible-consumption

A sigmoid regression and artificial neural network models for day-ahead natural gas usage forecasting

J. Ravnik [a,*], J. Jovanovac [b], A. Trupej [c], N. Vištica [d], M. Hriberšek [a]

[a] Faculty of Mechanical Engineering, University of Maribor, Smetanova Ulica 17, SI-2000, Maribor, Slovenia
[b] Plinacro d.o.o, Savska Cesta 88a, 10000, Zagreb, Croatia
[c] Energy Agency, Strossmayerjeva 30, 2000, Maribor, Slovenia
[d] Croatian Energy Regulatory Agency, Ulica Grada Vukovara 14, 10000, Zagreb, Croatia

ARTICLE INFO

Keywords:
Natural gas
Demand forecasting
Sigmoid regression
Neural networks
Genetic optimisation

ABSTRACT

Reliable and accurate day-ahead forecasting of natural gas consumption is vital for the operation of the Energy sector. Three different forecasting models are developed in this paper: The sigmoid function regression model, the feed-forward neural network, and the recurrent neural network model. The models were trained, compared, and validated using gas consumption data from 115 measuring stations in Slovenia and Croatia, which have been in operation for more than three years. The Genetic optimisation algorithm was used to train the neural networks and the Levenberg-Marquardt algorithm was used to obtain the parameters of the sigmoid model. The results show that both neural network models perform similarly, and are superior to the sigmoid model. The models were prepared for use in conjunction with a weather forecasting service to generate day-ahead or within-day forecasts, and are applicable to any geographical area. The neural network models achieve mean absolute percentage error between 5% and 10% in the entire temperature range. The sigmoid model reaches similar accuracy only for temperatures below 5°*C*, while for higher temperatures the error reaches up to 30%–40%.

1. Introduction

Modern society is dependent on natural gas as one of the main sources of energy. Since most natural gas is delivered to end users via pipelines, it is necessary to predict future gas demand as accurately as possible. The biggest challenge is to balance supply and demand for end users daily, with gas consumption having to be forecast accurately within one day and for the next day.

Attempts to use mathematical models to predict consumption began in the last century (Herbert (1987)). Since then, a wide range of models has been proposed by many authors. An overview prepared by Soldo (2012) shows a wide range of models such as the logistic curve model, the grey model, statistical models, econometric models, neural network models, genetic algorithms, mathematical models, the Hubbert curve model and their combinations. Soldo identified the approaches used by the researchers based on the forecast area (global, national, individual consumer), the forecast horizon (hourly, daily, monthly), the gas data measurements used and the model applied.

If a time series of gas consumption and outdoor temperature measurements is available, a forecast model can be developed in two ways. Focusing on the time series leads to ARIMA type approaches (Erdogdu (2010)) or to neural networks (Farzaneh-Gord and Rahbari (2018)), where taking several days' worth of input predicts the output for the next day. On the other hand, if one focuses on the relationship between gas consumption and temperature, one finds that it is *S*-shaped. The measurements show a constant high gas consumption at low temperatures, an almost linear decrease in consumption at moderate temperatures and a low constant consumption at high temperatures. This results in models based on *S*-shaped functions. A general term for *S*-shaped functions is the sigmoid function (Forouzanfar et al. (2010)). Some examples of sigmoid functions used in gas consumption modelling are the logistic function, the Gompertz function, the hyperbolic tangent and the arc tangent function.

In recent years, researchers have carried out studies with similar objectives, most of which have focused on a single country. In China, for example, Zeng and Li (Zeng and Li, 2016; Zeng, 2017) used a self-adjusting intelligent grey model to forecast natural gas demand, while Ma and Liu (2017) focused on the growth of annual natural gas

* Corresponding author.
E-mail addresses: jure.ravnik@um.si (J. Ravnik), josip.jovanovac@plinacro.hr (J. Jovanovac), aleksander.trupej@agen-rs.si (A. Trupej), nvistica@hera.hr (N. Vištica), matjaz.hribersek@um.si (M. Hriberšek).

https://doi.org/10.1016/j.clrc.2021.100040
Received 4 May 2021; Received in revised form 19 August 2021; Accepted 20 October 2021

consumption. They showed that predicting the behaviour of very large consumer groups using the grey model is accurate. They confirmed the well-known fact that predicting the total consumption of many consumers is more reliable than concentrating on a single consumer. Zhao and Wu (2020) proposed an adjacent accumulation grey model to forecasting non-renewable energy consumption in Asia-Pacific Economic Cooperation. Shaikh et al. (Shaikh and Ji, 2016; Shaikh et al., 2017) used optimised nonlinear grey models and logistic modelling analysis, while Zhang and Yang (2015) used the Bayesian model averaging. A model for short-term natural gas prediction using support vector regression was developed by Zhu et al. (2015). Bai and Li (2016) proposed a structure-calibrated support vector regression approach to predict daily natural gas consumption.

Day-ahead forecasting has been the focus of research by Panapakidis and Dagoumas (2017), who proposed a model using a combination of wavelet transform, genetic algorithm, and neural network techniques. They confirm that accurate forecasts of natural gas demand can be essential for utilities, energy traders, regulatory authorities and decision-makers. Short-term forecasting was the focus of the work of Yu and Xu (2014), who used a combination of optimised genetic algorithm and neural network techniques to develop a short-term load forecasting model for natural gas.

Akpinar et al. (2017) used neural networks and the sliding window approach for day-ahead natural gas demand forecasting. They report that although coding the training algorithm for neural networks is demanding and optimising the weights and biases takes considerable CPU time, the utilisation algorithm is relatively simple, and does not require large computational resources. The same research group (Akpinar et al., 2016) proposed forecasting natural gas consumption with hybrid neural networks — Artificial bee colony approach, and (Akpinar and Yumusak, 2019) studied forecasting daily and monthly demand for mid-term natural gas as contract estimations using other statistical methods, and (Akpinar and Yumusak, 2017) applied a navie approach using a sliding window. Chen et al. (2018) proposed a novel approach based on a nonlinear learning ensemble of time series predictions with deep learning, based on neural networks with long-term short-term memory, neural networks, a support vector regression machine and optimisation algorithms. Taspinar et al. (2013) used artificial neural networks (ANN) to predict the natural gas consumption in Turkey based on data from four years. Chen et al. (2020) proposed a hybrid forecasting model, Functional AutoRegressive and Convolutional Neural Network model for Germany. Szoplik (2015) produced a multi-layer perceptron model that uses data describing the actual natural gas consumption in Poland. Laib et al. (2019) confirmed that natural gas consumption can be predicted accurately using Recurrent Neural Networks by studying Algerian natural gas daily consumption profiles. Karabiber and George (2020) considered natural gas demand in Denmark, and found that solar radiation as an input parameter is ineffective in terms of predictive accuracy. Beyca et al. (2019) developed three models for Istanbul, based on multiple linear regression, an artificial neural network and support vector regression. They claim that support vector regression provides reliable and accurate results in terms of lower prediction errors for time series forecasting of natural gas consumption compared to the other two approaches.

Since the sigmoid function is nonlinear, a nonlinear fitting algorithm must be used to determine the model parameters. Siemek et al. (2003) used the Newton-Gauss algorithm to determine the model constants for the Hubbert model for modelling gas consumption in Poland. The Levenberg-Marquardt training algorithm was used to train an artificial neural network by Ivezic (2006) for gas consumption forecasts in Serbia.

Several other approaches were also used. Gascon and Sancez-Ubeda (2018) used generalised additive models for short-term natural gas demand forecasting. Aguilera and Ripple (2011) used the Variable Shape Distribution model to estimate the total stock of conventional gas in the Asia Pacific. Azadeh et al. (2015) proposed to use an integrated emotional learning fuzzy inference approach for optimal training of forecasting models for natural gas demand forecasting models. To optimise the natural gas supply in South America Chavez-Rodrigez et al. (2017) modelled the long-term natural gas dynamics by combining the LEAP (Long range Energy Alternatives Planning System) simulation model and the TIMES (The Integrated MARKAL-EFOM1 System) model.

A small number of studies were carried out in Slovenia and Croatia. Sabo et al. (2011) investigated natural gas consumption in Croatia based on hourly temperature and gas consumption measurements. Vištica et al. (2015) analysed the deviations between nominated and realised gas quantities for the balancing group consisting of 36 members in the Croatian gas market. Potočnik et al. (2007) examined the risks associated with forecasting models, and exposed the Slovenian model of economic incentives that motivates natural gas distributors to forecast their future consumption. Potočnik and Govekar (2010) presented practical results of forecasts for the natural gas market, and stressed the importance of including the right variables in the model and understanding the underlying principles of energy consumption correctly. Potočnik et al. (2014) also considered the short-term natural gas forecast for households in Croatia. The same research group investigated the influence of solar radiation on gas forecasting models (Soldo et al., 2014). Karasalihovic et al. (2003) investigated the Croatian gas market and found a strong correlation with the Gross Domestic Product. Ravnik and Hriberšek (2019) proposed a methodology for short-term forecasts in Slovenia based on the sigmoid-type model. Hribar et al. (2019) focused on the gas use of the Slovenian capital Ljubljana by looking at different machine learning models, such as linear regression, kernel-machine and artificial neural networks. The recurrent neural network and the linear regression model proved to be the two most accurate models.

The motivation for developing short-term gas demand forecasts in countries that import most of their natural gas is twofold. First, to avoid the additional costs associated with ordering too little or too much gas in the market, the day-ahead forecast can be used to predict the gas usage in the next day. Second, since a typical country distributes gas on its territory across several suppliers, it is important to have a simple algorithm combined with a forecasting method to divide gas provisionally between the suppliers. With a well-defined forecasting method, published in the legislation, a consistent, fair and reliable model for preliminary allocation of gas consumption is available. Due to their simplicity of having only 4 parameters defining the model, sigmoid regression models have been popular (Ravnik and Hriberšek, 2019), and were implemented in the legislative framework. Although they are simple, the predictive power of regression is expected to be low compared to artificial neural networks.

In this paper we develop models that are geared to day-ahead and within-day forecasting of gas demand based on gas consumption measurement in Slovenia and Croatia. The predictions are made at the consumer level, and give gas utilities the ability to predict the behaviour of all customers in their portfolio. Three model types are considered: The sigmoid-type power law model, the Feed-Forward Neural Network (FFNN) model and the Recurrent Neural Network model (RNN). We compare the sigmoid model with the neural network model to determine the advantages and disadvantages of both approaches, due mainly to the prediction accuracy, but also with respect to the required computational resources and ease of implementation. So far, no studies comparing the characteristics of Slovenian and Croatian gas consumers as presented in this paper have been conducted, although Slovenia and Croatia are neighbouring countries.

The original contribution of this paper consists of three parts. First, we present three models for the short-term (day-ahead and within-day) prediction of gas consumption. The developed models are compared, and their advantages are shown. The models can be used internationally for any gas forecasting study. Secondly, we identify the best models, and present their effectiveness using a data set consisting of 115 measuring stations and more than one million daily gas consumption measurements. Finally, we present the results of the comparison of the Slovenian and Croatian gas consumption characteristics, and the comparison between the modelling of individual consumers and the modelling of hydraulic cells covering a large number of consumers.

2. The data set

We developed the models based on daily gas consumption and temperature measurements in Slovenia and Croatia. The Croatian data set consisted of measurements on 18 hydraulic cell groups in Croatia in the period 1.1.2015–30.4.2019. These data sets were named $\mathcal{D}_1$, … $\mathcal{D}_{18}$. They correspond to geographical regions with similar climate characteristics, and consist of daily measurements of gas consumption in 126 hydraulic cells. Each hydraulic cell includes several consumers of different types. The measurements were performed by the Croatian Energy Regulatory Agency. For each group a representative meteorological station was selected, from which temperature measurements were taken. The map of locations of hydraulic cells and meteorological stations is shown in Fig. 1. In total there were 27,782 days with data from Croatia from 18 groups formed around meteorological stations (see Fig. 2). The 18 Croatian data sets thus represent daily sums of gas consumption for a large number of individual consumers.

In contrast, in Slovenia, we considered individual consumers. The consumption data were data obtained from 97 gas measuring stations located at individual consumers, such as residential houses and small businesses in the period 3.9. 2009 - 30.5.2013. Based on the location of the measuring station, the temperature measurements were carried out at the nearest representative meteorological station. These data sets were named $\mathcal{D}_{19}$, … $\mathcal{D}_{115}$.

The measurements were taken by the Energy Agency of the Republic of Slovenia by performing hourly gas consumption measurements at 260 consumers (end users) in Slovenia. At the same time, 18 meteorological stations recorded climate conditions. For each of the 260 consumers, 32,856 hourly measurements were made during the observation period. The consumers were chosen in such a way that they represented several consumer groups, and were representative of their type of activity (e.g. Agriculture, Civil Engineering, Residential, etc.). The consumer groups are defined in the standardised Business Registry. Secondly, consumers were chosen in such a way that they were located in different local climate regions of the country.

Given the gas consumption dataset, we first performed a statistical analysis to determine the consumption variation within the dataset. For each consumer we calculated the average daily consumption and Standard Deviation. In order to exclude erroneous gas consumption data, the measurements that exceeded the 7σ interval were eliminated from the dataset. In total 0.03% of all measurements were rejected. We chose 7σ to be sure, that the rejected data points did not represent valid measurements. Furthermore, due to equipment failure or other unforeseen circumstances, all of the consumers did not have a complete four-year dataset of the measurements available. The majority of the consumers had between 70% and 90% of the maximum number (each day with a full 24-h resolution) of measurements. Finally, several consumers used natural gas for process purposes in a non-temperature dependent manner. We chose 97 consumers with more than a 1000 days of measurements to be included in this analysis. The total number of days with measurements was 119,045. The map of Slovenia, with locations of cities where measurements took place and meteorological stations is shown in Fig. 1. The number of days with data is shown in Fig. 2.

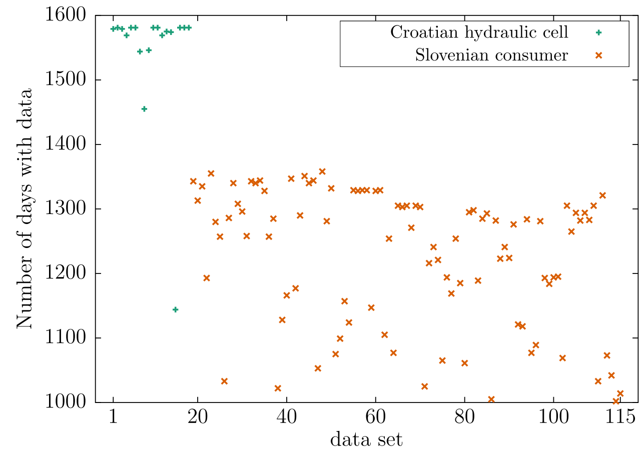

Fig. 2. The number of days with data for all of the 115 data sets.

In (Ravnik and Hriberšek, 2019) it was shown that, although the market gas price shows some fluctuations over the measurement period, we did not observe a strong correlation between price and consumption. Furthermore, we assumed that the fluctuation of the natural gas price during the measurement period was small compared to the Gross Domestic Product of Slovenia and Croatia, which is why the natural gas price was not considered as a variable in the modelling. Although there is a tendency to reduce heat losses from residential buildings, we believe that this does not have a significant impact on natural gas consumption. Thus, we may assume that the consumption characteristics have not changed during the observation period. For all 115 data sets we used the last 365 measurement days as the validation data set, and used only the remaining measurements for model development.

The forecasting task discussed in this paper is a short-term forecast for one day in the future. Based on the measurements collected on this day, and on several days before, a forecast is made of gas consumption on a single day in the future. To put this methodology into practice, we

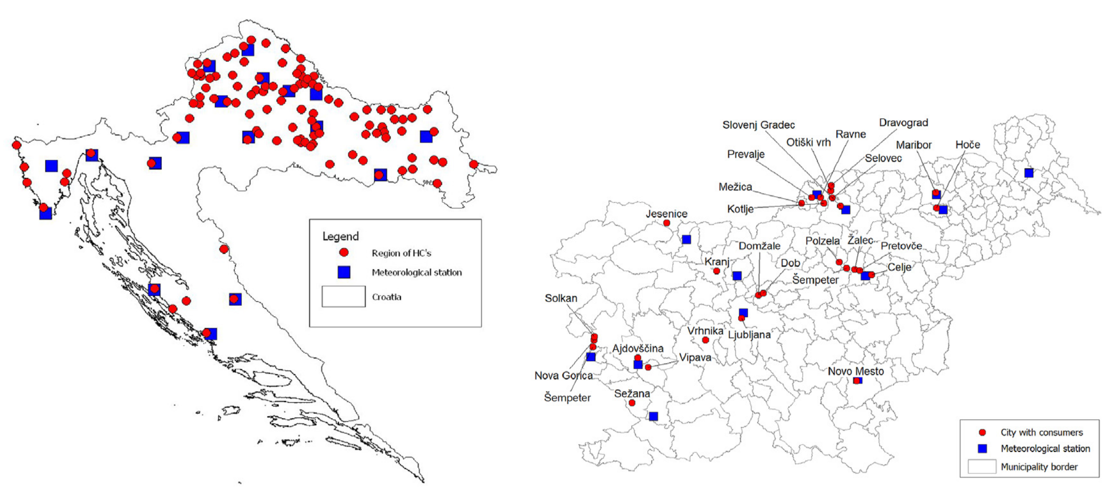

Fig. 1. Maps of Croatia (left) and Slovenia (right) with location of meteorological stations and gas consumers. In Croatia hydraulic cells are shown, in Slovenia cities where measurements took place are shown.

recommend using the Weather Service with hourly forecasts for all regions of both countries. In Slovenia and Croatia the gas day is defined as the period between 6 a.m. on that day and 6 a.m. on the next day. It is, therefore, possible to use the models developed below as follows. After 6 a.m. the gas consumption measurements of the previous day are available. In addition, the Weather Service has prepared temperature forecasts for the following gas day, which allowed the models to be used and the gas consumption forecast to be made. These data can be used to allocate gas consumption preliminarily between the suppliers. If necessary, the same model can be used again later in the day, in conjunction with additional measurements already available. The actual times of day at which the model is used will depend on the Regulations of a particular country.

The inputs for the forecasting models considered in this paper are the gas consumption in a gas day and average temperature in a gas day. The average temperature is calculated by averaging the measured or forecast hourly temperatures during a gas day. In (Ravnik and Hriberšek, 2019) a distinction has been made between weekends, holidays and workdays. It was concluded that such a distinction does not contribute significantly to forecasting accuracy, so, in this work, we treat all days equally.

3. The sigmoid model

The sigmoid gas consumption model, which connects the average outside temperature and gas consumption, is defined using the following formula (Ravnik and Hriberšek, 2019):

$$P_j = \max\left\{P^m\left[\frac{A}{1+\left(\frac{B}{T_j-40}\right)^C}+D\right],0\right\} \tag{1}$$

where P_j is the estimated gas consumption for gas day j, P^m is the average daily gas consumption of the consumer for which the estimate is made, A, B, C and D are the model parameters, and T_j is the average gas day temperature on day j in $^\circ C$.

Different values of the parameters A, B, C and D result in different consumption curves. To develop a numerically stable algorithm for determining the sigmoid curve parameters A, B, C and D, we first normalised the gas consumption in each data set with $P^m = \frac{1}{N}\sum_{j=1}^{N} P_j^m$, where N is the number of data points in the data set.

The optimal values of parameters A, B, C and D were determined by nonlinear fit of the sigmoid curve to the data sets minimising the sum of square differences between the curve and the data points. To find the parameters we used the Levenberg-Marquardt method (Press et al. (1997)). The solution was found in an iterative manner using 10^{-6} as the convergence criterion. The initial values of parameters were: $A = 1$, $B = -30$, $C = 10$, and $D = 0.1$. The list of all parameter values for all data sets is given in the Appendix. The medians, obtained by considering all 115 data sets, are $A = 2.91$, $B = -36.46$, $C = 5.493$ and $D = 0.153$. The median sigmoid features low and constant gas usage at temperature above $20^\circ C$, an approximately linear increase of usage between $20^\circ C$ and $0^\circ C$, and slowing of increase of usage in the negative temperature range.

When applying the sigmoid curve for gas consumption forecasts, it is important that the available gas consumption data cover the entire temperature range typical for a specific geographical region in which the target consumer is located. With regard to the accuracy of the sigmoid approximation, it is also important that there is a comparable number of data points in the low and high temperature range, as only a few data points would not be able to ensure a representative functional dependence in this temperature range. With the effects of global warming, the availability of gas consumption data in the low temperature range is becoming scarce, but this does not mean that severe low-end temperatures are not to be expected in the future. In order to overcome this problem, consumption data should be used over a longer period of time, increasing the probability of collecting days with lower temperatures.

4. The artificial neural network models

In the following we develop day-ahead forecasting models based on a feed-forward neural network and recurrent neural network designs.

4.1. The feed-forward neural network

An artificial neural network consists of several layers containing information and connections between them. It supports any length of input and output layers. In our case, we selected the output layer as a single value - the predicted gas consumption P_j. As input we could have chosen only one value - the average temperature on the gas day for which we want to predict the gas consumption T_j. This would result in a model that would behave similarly to the sigmoid model presented above, for a known average temperature the model would predict the gas consumption. However, since the artificial neural network can take several values as input, we decided to include the gas consumption and the average temperature on the previous days as well. The reason for this decision is based on the fact that gas consumption on a given day depends on the average temperature and gas consumption on the previous days. For example, gas consumption on a cold day will be lower if the previous days were warm, and higher if the previous days were cold. In the models presented below, the size of the input layer is always odd. It consists of the average temperature on the day for which we want to predict the gas consumption T_j, and pairs of average temperature and gas measurements for n of the previous days. For example, if the input layer size is 5, it will consist of T_j, P_{j-1}, T_{j-1}, P_{j-2}, and T_{j-2}. With such an arrangement it is possible to train the neural network to recognise patterns in the gas consumption profile of the consumer and, thus, to predict gas consumption more successfully.

The artificial neural network consists of nodes distributed in layers (Bell, 2015). The values of the nodes for each layer are stored as vectors, i.e. n_i, where i is the layer number. The zeroth layer n_0 represents the input to the neural network. σ_i is an activation function used for the layer i. b_i are scalar values called bias. W_i are weight matrices. The number of rows in W_i is equal to the number of nodes in the n_i layer, the number of columns in the W_i matrix is equal to the number of nodes in the n_{i-1} layer. In this work, we use the sigmoid $\sigma(x) = (1+\exp(-x))^{-1}$, the hyperbolic tangent $\sigma(x) = \tanh(x)$ and the identity $\sigma(x) = x$ activation functions. The input is propagated through the network to the output layer by a sequence of the following algebraic expressions using the weights and biases of the network. Let the number of layers in the network be $k+1$ and so the output layer is n_k. Its value is estimated using

$$n_k = \sigma_k\Big(b_k + \cdots + W_4\sigma_3\Big(b_3 + W_3\sigma_2\Big(b_2 + W_2\sigma_1\Big(b_1 + W_1 n_0\Big)\Big)\Big)\Big) \tag{2}$$

To become useful, the neural network must be trained, i.e. we must find the optimal values for weights and biases based on the gas consumption measurements available in each data set. We transform the data set into training pairs. Suppose t_0 is the input layer of average temperature and gas consumption measurements in the days before the day for which we predict gas consumption, and t_k is the output layer, i.e., the measured gas consumption. If t_0 is used at the input, the neural network (2) creates the output n_k. We define the error vector for the output layer as $e_k = t_k - n_k$ where n_k is the output of the network, based on the input $n_0 = t_0$. Next, we define the L_2 error norm of the neural network for a single training pair as

$$L_2 = e_k \cdot e_k \tag{3}$$

For each data set we posses a certain number of training pairs N, $t_0^{(l)}$ and $t_k^{(l)}$, where l denotes the training pair number. Finally, we define the error of the neural network via the following norm

$$E = \frac{1}{N}\sum_{l=1}^{N} L_2^{(l)} = \frac{1}{N}\sum_{l=1}^{N}\left(t_k^{(l)} - n_k^{(l)}\right)^2, \tag{4}$$

where $n_k^{(j)}$ is obtained by propagating $n_0^{(j)} = t_0^{(j)}$ through the network. When training the network, our task is to minimize E by choosing an appropriate network structure (number and size of layers and activation function types), and then finding the optimal weights and biases.

4.2. Recurrent neural network model

When using FFNNs, as described above, we treat all inputs independently. Recurrent Neural Networks (RNNs) try to take advantage of the fact that we are dealing with inputs that are given in a temporal sequence. RNNs exploit the temporal relationship between inputs and outputs to produce better forecasts. RNNs are called recurrent because they perform the same task for each element of a time sequence, with the output depending on the previous calculations. RNNs can use information in sequences of any length, but in practice they are limited to looking back only a few steps. The following steps are necessary to perform the forecast:

$$\begin{aligned} h_{t-2} &= \sigma_{t-3}(Wh_{t-3} + Ux_{t-2}) \\ h_{t-1} &= \sigma_{t-2}(Wh_{t-2} + Ux_{t-1}) \\ h_t &= \sigma_{t-1}(Wh_{t-1} + Ux_t) \\ y_t &= \sigma_t V h_t \end{aligned} \tag{5}$$

The output y_t is generated by using a time series of the inputs x_t, x_{t-1} and x_{t-2}. This is done using a series of hidden layers h_t, …, h_{t-3}, activation functions σ_t, …, σ_{t-3} and weight matrices U, V and W. The deepest hidden layer $h_{t-3} = 0$ is normally set to zero. Several choices are available for the activation functions, such as the sigmoid, hyperbolic tangent or ReLU. The size of the input is n_x and the size of the output is n_y. The sizes of the hidden layers are all the same, n_h. The weight matrices have the following sizes: $U(n_h, n_x)$, $V(n_y, n_h)$ and $W(n_h, n_h)$. They must be determined using an optimisation strategy based on the available training data.

4.3. Model quality assessment measures

In order to have a mathematically based assessment of the quality of the developed models, the square of the sample Pearson correlation coefficient, denoted by r^2, was employed (Hellwig, 2003):

$$P = \sum_{j=1}^N P_j, \qquad P^m = \sum_{j=1}^N P_j^m, \qquad r^2 = \frac{\left(\sum_{j=1}^N P_j P_j^m - NP\,P^m\right)^2}{\left(\sum_{j=1}^N (P_j)^2 - NP^2\right)\left(\sum_j (P_j^m)^2 - NP^{m2}\right)}. \tag{6}$$

Here P_j is the forecast gas consumption for a consumer on the day j, while P_j^m is its measured counterpart, and $N = 365$ is the number of data points in the validation data set. The coefficient r^2 is the square of the covariance of the forecast and measured gas usage divided by the product of their Standard Deviations. It takes values between 0 and 1, with a higher value describing a better fit. The validation data set was not used in the model development, and consisted of the last 365 measurements taken for each individual data set. To further expose the difference between the forecast and measured gas usage, we use the relative RMS norm

$$RMS = \left(\frac{\sum_{j=1}^N \left(P_j - P_j^m\right)^2}{\sum_{j=1}^N \left(P_j^m\right)^2}\right)^{\frac{1}{2}}. \tag{7}$$

The RMS norm measures the difference between the model forecasts and measurements, with a smaller value indicating better agreement between the model and the measurements. Finally, the Mean Absolute Percentage Error (MAPE) is defined as

$$MAPE = 100\% \cdot \frac{1}{N} \sum_{j=1}^N ||1 - \frac{P_j}{P_j^m} \tag{8}$$

is also used to express the average expected forecast error of a single daily forecast. MAPE gives the difference between the measurements and forecasts in percentage of the measured value.

4.4. Genetic optimisation strategy

In the study we consider different designs of the neural networks in terms of the size and content of the input layer and the number and size of hidden layers. The output is, in all cases, the forecast gas consumption. We denote the ANN designs as $\mathcal{Z}_Y^{xW}$, where Z is $\mathcal{F}$ for the feed-forward network and $\mathcal{R}$ for the recurrent network, X is the number of gas measurements on the previous days used in the input, Y is the number of average temperatures used in the input, W stands for the size and number of hidden layers, and x for the type of activation function used (s for sigmoid $(1 + \exp(-x))^{-1}$ and t for tanh). For example, considering day j, the feed forward network $\mathcal{F}_4^{s5,5}$ has the following data in the input layer P_{j-1}^m, P_{j-2}^m, P_{j-3}^m, T_j, T_{j-1}, T_{j-2}, T_{j-3}, and two hidden layers of size 5 with a sigmoid activation function. The output of the network is always the predicted gas consumption for the day j: P_j. The activation function for hidden layers was the sigmoid or tanh, and for the output layer the identity function.

The total number of weights and biases can be determined from the structure of the network and, for the networks used in this study, is in the range between 26 for a network with 3 inputs and 1 hidden layer of size 5, 56 for a network with 9 inputs and 1 hidden layer of size 5, and 76 for a network with 7 inputs and 2 hidden layers of size 5.

We used the genetic optimisation algorithm to find the optimal values for weights and biases for each data set and for each neural network design. Let us consider a gene as a single value of a weight or bias in the neural network. The entire network is defined as a collection of genes that we call a chromosome. A population is a collection of M chromosomes. Starting from the definition of the L_2 norm, we define the following quantities for the i-th chromosome:

$$F_i = \frac{1}{1 + L_{2,i}}, \qquad F = \sum_{i=1}^M F_i, \qquad C_i = \sum_{j=1}^i \frac{F_j}{F}, \tag{9}$$

where F_i is the fitness for the i-th chromosome, F is the total fitness, C_i is the chromosome cumulative probability, and $L_{2,i}$ is the L_2 norm (3) of the i-th chromosome. Genetic optimisation is based on two additional user defined parameters: The cross over rate ζ and the mutation rate μ. The selection of fit chromosomes is performed using eq. (9). Crossover between two fit chromosomes is implemented by choosing genes from both chromosomes randomly. Mutation changes μ genes randomly.

For the genetic optimisation of weights and biases in the neural networks we used the population size $M = 200$, the number of iterations $n = 10^5$, the crossover rate $\zeta = 0.9$ and the mutation rate $\mu = 0.2$. The search space for weights and biases was $(-2.5, …, 2.5)$.

5. Results

The 115 data sets were modelled with both the sigmoid and the artificial neural network models. The results are given below.

5.1. Determination of optimal neural network setup

First, we investigated the effect of the structure of the artificial neural network on the predictive power of the ANN models. In Fig. 3 we show the square of the Pearson sample correlation coefficient for a selected group of data sets. The data sets have been selected so that some have the expected gas consumption - average temperature dependence - and others do not. In the case where the gas is used temperature-dependently, we observe the values of the square of the Pearson sample correlation coefficient close to one, meaning that the ANN describes the data well. Looking at the square of the Pearson sample correlation coefficient plots, we observe that different ANN designs yield results of the same order of magnitude. Nevertheless, such comparison reveals the optimal neural network design.

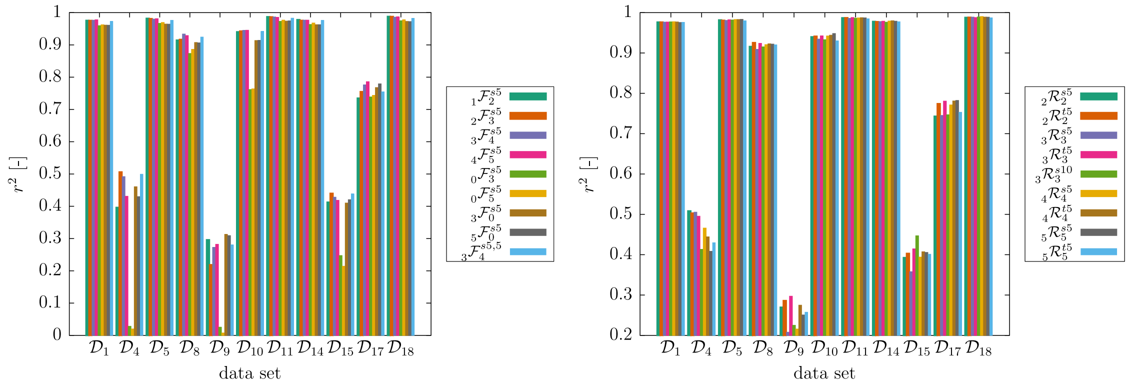

Fig. 3. Comparison of the square of the Pearson sample correlation coefficient obtained using different artificial neural network designs: FFNNs (left) and RNNs (right).

In data sets where gas was not used in a temperature dependent manner ($\mathcal{D}_4$, $\mathcal{D}_9$ and $\mathcal{D}_{15}$) the neural networks taking only temperature as input ($\mathcal{F}_3^5$ and $\mathcal{F}_5^5$) fail. The other designs are comparable, albeit the forecasting accuracy is low. The feed forward networks performed better then recurrent networks in these cases.

We were interested in discovering the neural network design which preforms best when temperature dependent data are considered. Considering data sets $\mathcal{D}_1, \ldots, \mathcal{D}_{18}$ with $r^2 > 0.9$, we compared the neural network designs in Fig. 4. The comparisons was made in the following way. For each data set we identified the best neural network design, i.e. the one with the largest values of square of the Pearson sample correlation coefficient. For each neural network design we present in Fig. 4 the average difference between the max r^2 calculated using all data sets.

Fig. 4 shows that all ANNs perform better than the sigmoid curve model. Designs that consider only gas consumption or only temperature perform poorly. A comparison of the recurrent and feed-forward networks shows that both can achieve a similar level of accuracy, but the RNNs seem to be slightly better.

Altogether the best feed forward design is $\mathcal{F}_4^{s5}$ and the best recurrent design is $\mathcal{R}_5^{s5}$. Based on this analysis, we selected these two designs for all further analyses. The feed forward network $\mathcal{F}_4^{s5}$ has the size of the input layer 7, so in order to forecast gas usage on day j: P_j we require 7 data points: The average temperature on the same day T_j, as well as the average temperature and gas usage for the three previous days: T_{j-1}, P_{j-1}^m, T_{j-2}, P_{j-2}^m, T_{j-3}, P_{j-3}^m. The recurrent network $\mathcal{R}_5^5$ uses $T_j, \ldots, T_{j-4}$ and uses $P_{j-1}^m, \ldots, P_{j-5}^m$. Both use the sigmoid as the activation function.

5.2. Comparison of developed models

Secondly, we modelled all 115 data sets with the sigmoid curve model, feed forward neural network model $\mathcal{F}_4^{s5}$ and the recurrent neural network model $\mathcal{R}_5^{s5}$. The square of the Pearson sample correlation coefficient and the RMS norms are shown in Fig. 5. Several observations can be made. The sigmoid curve model and the ANN models behave similarly, resulting in the square of the Pearson sample correlation coefficient and the RMS norm of the same order of magnitude. Nevertheless, it can be observed that the artificial neural network models outperformed the sigmoid model in all cases. Even though the computational resources required for training the artificial neural network are much larger than

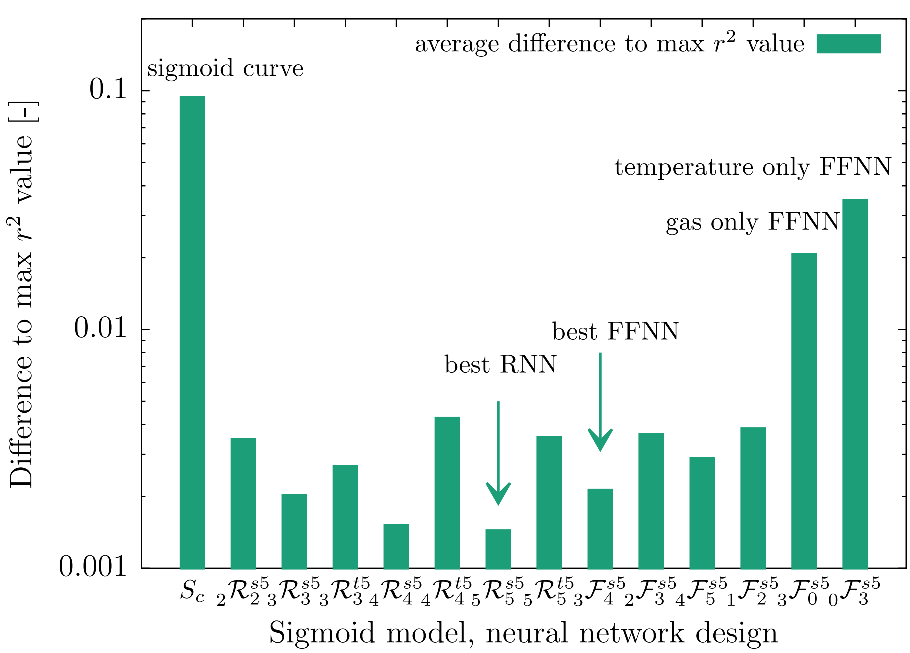

Fig. 4. Comparison of the sigmoid model and different neural network designs. The values on the ordinate reveal the average difference between an individual model and the best model.

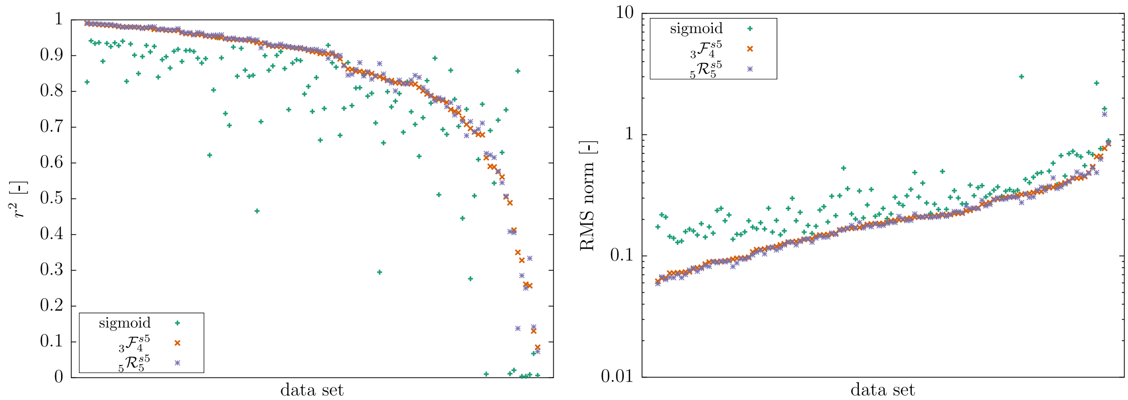

Fig. 5. Comparison of square of the Pearson sample correlation coefficient (left) and the RMS norm (right) for the sigmoid and artificial neural network models for all 115 gas usage measurement data sets. The data sets were sorted to improve the readability of the plots.

the resources needed to estimate the sigmoid model parameters, they are still manageable, so we recommend using the artificial neural network models in practical applications.

Comparing the performance of the feed-forward and recurrent neural networks, we observe that they performed similarly, with the slight advantage of the recurrent neural network. The differences in results are most prominent for data sets which were captured poorly ($r^2 < 0.9$). For data sets having ($r^2 > 0.9$) we observed an almost identical performance of the FFNN and RNN.

Examining the square of the Pearson sample correlation coefficient for neural network models (left panel in Fig. 5), we can divide the developed models into three categories. In the first category we place the good models ($r^2 > 0.9$), in the second fair models ($0.5 < r^2 < 0.9$) and in the last category we place poor models ($r^2 < 0.5$). We find more than half (56%) of the models in the good model category, 37% in the fair model category, and only 7% of the models in the bad category. The RMS norm results (right panel in Fig. 5) reveal that the neural network models outperformed the sigmod model in all data sets.

To examine the origin of the prediction accuracy for all three types of models, we take a closer look at two data sets that were modelled very

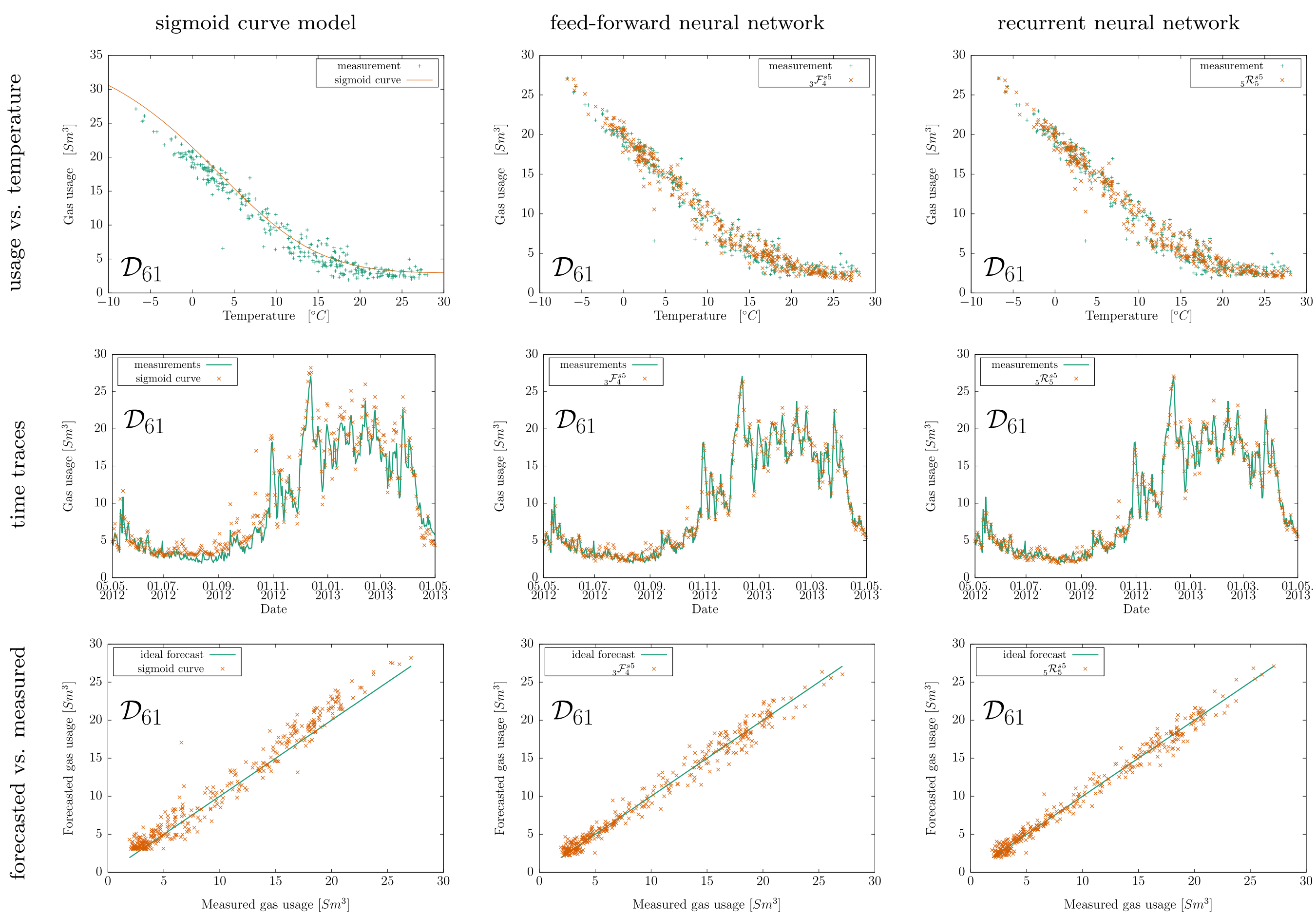

Fig. 6. Gas usage measurements and model forecasts shown as gas usage versus average gas day temperature plots (top) and time traces (middle) and forecasted versus measured gas usage (bottom) for data set $\mathcal{D}_{61}$. Results of sigmoid curve model are in left panels, FFNN in center panels and RNN in right panels.

successfully or very poorly. In Fig. 6 we take a detailed look at the results of a single data set, $\mathcal{D}_{61}$, which was modelled very successfully by all three approaches. The square of the Pearson sample correlation coefficient was $r^2 = 0.935$ for the sigmoid curve model, $r^2 = 0.983$ for the feed-forward neural network and $r^2 = 0.984$ for the recurrent neural network model. Even though the $\mathcal{D}_{61}$ data set had a very typical consumption-versus-temperature relationship and the sigmoid model captured it well, it was inferior to both neural network models. The difference was more pronounced when more challenging data sets are considered, for example, $\mathcal{D}_{110}$ (Fig. 7). In this case we observe that the sigmoid curve model was not capable of capturing the large gas consumption variation well at a given temperature. The data set contained up to 500% change in gas consumption at temperatures between $0°C$ and $10°C$, and exhibited non-temperature dependent behaviour. As a result, the square of the Pearson sample correlation coefficient for the sigmoid model was $r^2 = 0.738$. Both neural network models performed much better, reaching $r^2 = 0.947$, and demonstrating the ability to detect consumption behaviour that is only partially temperature dependent. Understandably, the performance of the neural network was worse compared to the $\mathcal{D}_{61}$ dataset.

It is worth pointing out that neural network performance for the non temperature dependent dataset $\mathcal{D}_{110}$ was better than the sigmoid model performance on the well behaved dataset $\mathcal{D}_{61}$. When the models developed in this paper will be used by gas supplier companies they will be used to forecast gas usage of a very large number of consumers. The behaviour of the consumers is expected to be primarily temperature dependent, although some deviations from this behaviour may occur. The 115 gas measuring stations used in this study were chosen in such a way that they represent a good sample of gas usage behaviour in Slovenia and Croatia. The model which will be chosen for daily use is expected be able to forecast gas usage for a wide variety of gas users. The final example, which undoubtedly proves that neural network models are superior to the sigmoid model, is shown in Fig. 8, where data set $\mathcal{D}_{45}$ is analysed. This dataset exhibits two behaviours clearly - a temperature dependent and a non-temperature dependent behaviour. Analysing it, we find that the reason for poor performance of the sigmoid model comes from the fact that gas was used in two different regimes in the temperature range $10°C < T < 15°C$. The sigmoid model cannot capture both regimes at the same time, while the neural network models can. The neural network models reach $r^2 = 0.99$, which is a very good result.

In this context it should be noted that the performance of the neural network for the non-temperature dependent data set $\mathcal{D}_{110}$ was better than the performance of the sigmoid model for the well behaved dataset $\mathcal{D}_{61}$. If the models developed in this paper are used by gas supply companies, they will be used to predict gas consumption of a very large number of consumers. It is expected that the behaviour of the consumers is primarily temperature dependent, although some deviations from this behaviour may occur. The 115 gas metering stations used in this study were selected to provide a good example of gas consumption behaviour in Slovenia and Croatia. It is expected that the model chosen for daily use will be able to forecast gas consumption for a wide range of gas consumers. The last example, which proves beyond doubt that neural network models are superior to the sigmoid model, is shown in Fig. 8, where the data set $\mathcal{D}_{45}$ is analysed. This data set shows two types of behaviour clearly - one temperature-dependent and one non-temperature-dependent behaviour. When we analyse it, we find that the reason for the poor performance of the sigmoid model is that the gas was used in two different regimes in the

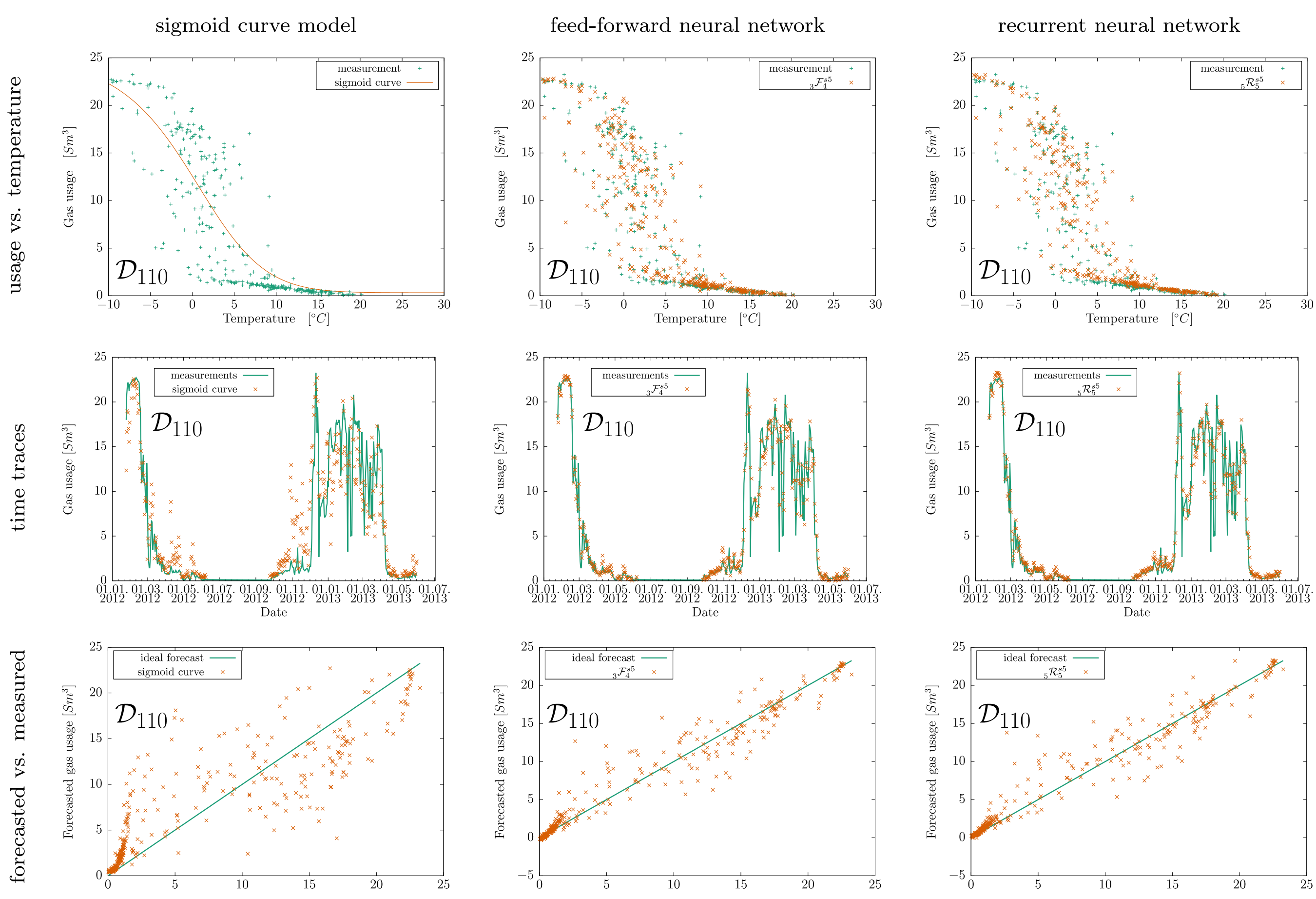

Fig. 7. Gas usage measurements and model forecasts shown as gas usage versus average gas day temperature plots (top) and time traces (middle) and forecasted versus measured gas usage (bottom) for data set $\mathcal{D}_{110}$. Results of sigmoid curve model are in left panels, FFNN in center panels and RNN in right panels.

$10^{\circ}C < T < 15^{\circ}C$ temperature range. The sigmoid model cannot capture both regimes at the same time, while the neural network models can. The neural network models reached $r^2 = 0.99$, which is a very good result.

Finally, we analyse mean average percentage errors (8) for the three developed models. In Fig. 9 we show MAPE of the forecasted gas usage versus temperature for four data sets, which were modelled successfully (ANN square of the Pearson sample correlation coefficient $r^2 > 0.98$). When comparing the sigmoid model and the neural network models, we find that the ANN errors are lower, and that the difference between the two modelling approaches is the largest in the mid temperature range ($8^{\circ}C$–$18^{\circ}C$). This means that the sigmoid model only works at low temperatures ($< 5^{\circ}C$). It is clear that the neural network models are superior in the entire temperature range. Comparing the feed-forward and recurrent neural networks, we observe similar performance but notice that, in most cases the MAPE for the recurrent model are the lowest. ANNs reach MAPE similar to that reported by Akpinar et al. (Akpinar and Yumusak, 2017), in the order of 5%–10%.

In Fig. 10 we show the ratio of MAPE of the neural network and the MAPE of the sigmoid model for all data sets (left panel), and examine its correlation with the square of the Pearson sample correlation coefficient (right panel). We observe, since all ratios in the plot are less than one, that both feed-forward and recurrent neural network models have a smaller MAPE compared to the sigmoid model. For about one half of the data sets the neural network error is less than 60% of the sigmoid model error. For the other half, the improvement of neural network models over the sigmoid model is smaller, but still there.

The improvement of ANN over the sigmoid model was best for data sets with a higher square of the Pearson sample correlation coefficient (right panel of Fig. 10), which means that forecasting of well-behaved temperature-dependent gas consumers is greatly improved when the sigmoid model is replaced by the neural network model.

5.3. Application of the developed models

Based on the presented results, the following methodology should be employed to produce day-ahead forecast of gas consumption and preliminary allocation of gas between consumers.

- The gas distribution network in an area should be divided into smaller regions with similar climate characteristics, for which weather forecasts are made regularly and are accessible. For the easiest implementation, a contract with the Weather Service is advisable, which enables the automatic exchange of data. The regions can be centred around meteorological stations, so minimal distance between consumers and temperature measurements is achieved.
- Measurements of gas consumption at individual consumers or at a hydraulic cell level must be recorded daily for a period of at least three years. It is recommended to select metering points (reference consumption points) for various consumers according to the purpose of their gas consumption.
- We recommend training of a recurrent neural network using this design: $\mathcal{R}_5^{s5}$. After initial training, the gas usage measurements should continue on reference consumption points, and the network should be re-trained once per year when new measurements become available.
- The trained neural networks can then be used daily when new temperature forecasts become available. When they are applied for

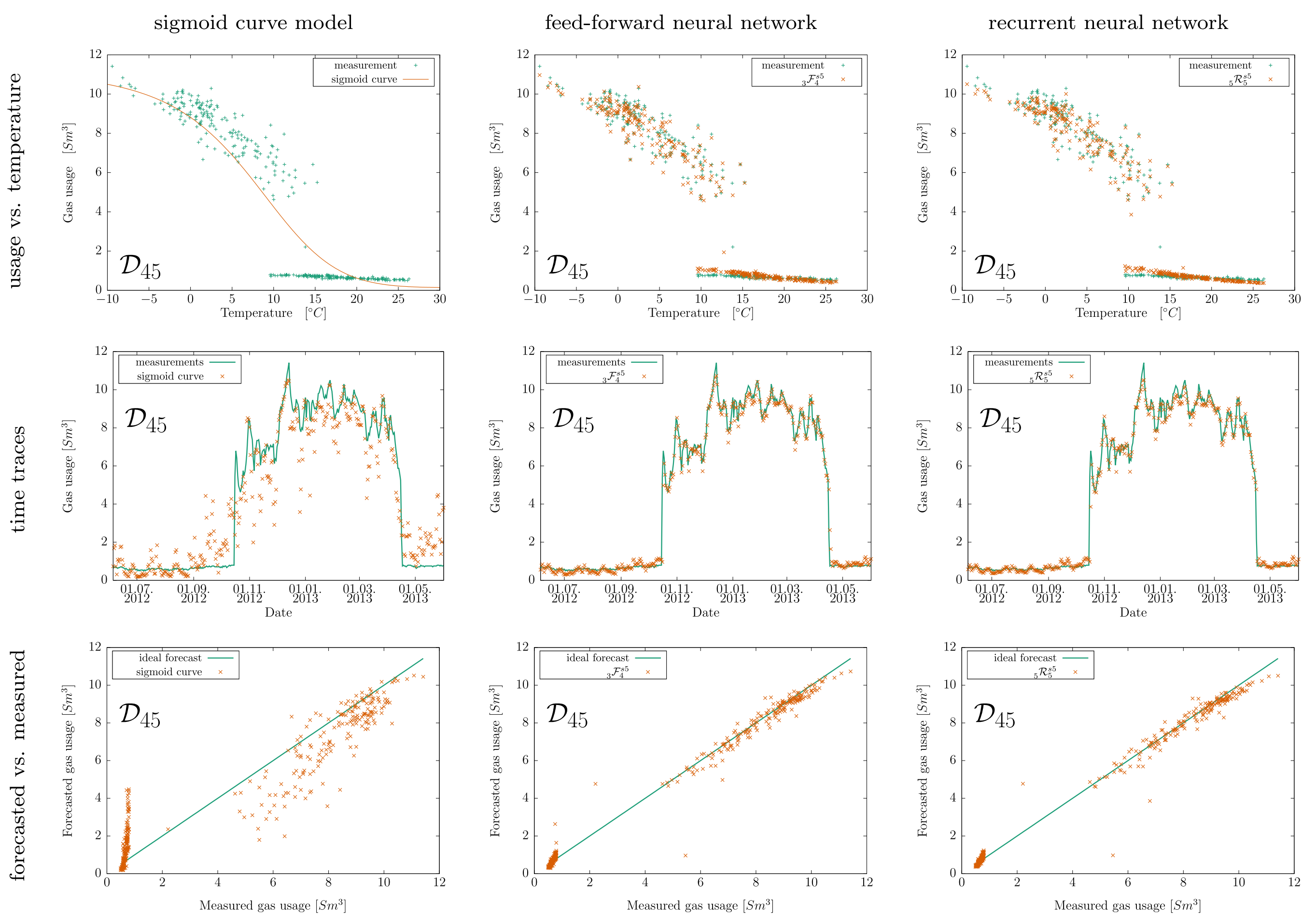

Fig. 8. Gas usage measurements and model forecasts shown as gas usage versus average gas day temperature plots (top) and time traces (middle) and forecasted versus measured gas usage (bottom) for data set $\mathcal{D}_{45}$. Results of sigmoid curve model are in left panels, FFNN in center panels and RNN in right panels.

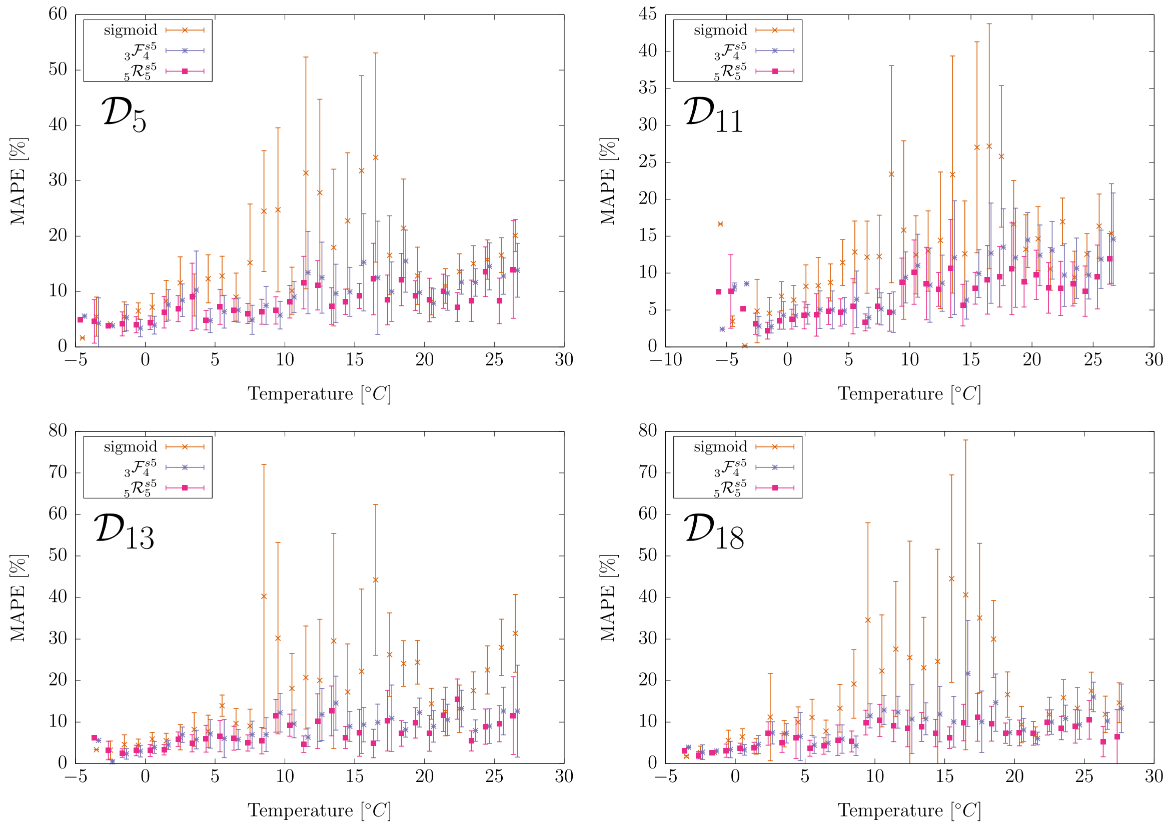

Fig. 9. MAPE of the forecasted gas usage expressed in percent versus temperature for four data sets: $\mathcal{D}_5$, $\mathcal{D}_{11}$, $\mathcal{D}_{13}$ and $\mathcal{D}_{18}$, which were successfully modelled (ANN square of the Pearson sample correlation coefficient $r^2 > 0.98$). The error bars represent the 95% confidence interval. The sigmoid model, the feed-forward neural network $\mathcal{F}_4^{s5}$ and the recurrent neural network $\mathcal{R}_5^{s5}$ are shown. The poor performance of the sigmoid model in the medium temperature range (8°C–18°C) is obvious.

individual consumers, the results must be scaled in proportion to the individual consumer's annual gas usage.

- When the total gas consumption for a hydraulic cell in the gas distribution network is known, it is necessary to make a preliminary allocation of the gas consumption of each consumer based on the application of the models. This provides a unified and equitable way of determining the preliminary allocation, and, when introduced into the regulatory framework, ensures smooth operation and helps to avoid conflicts between gas suppliers. We assume that the total amount of gas consumed is measured in a hydraulic cell S. Then, this gas quantity must be divided among the consumers. A forecast is made for each of the consumers. Let the number of consumers be n and the predicted gas consumption of the $i-th$ consumers be P_i. Due to the inaccuracy of the forecast, we find that the total measured gas consumption is not equal to the sum of all forecasts for all consumers, $\sum_{i=1}^{n} P_i \neq S$. We want to compute the preliminary gas consumption distribution A_i such that $\sum_{i=1}^{n} A_i = S$. To achieve this, the preliminary gas consumption allocation A_i is calculated using the following formula:

$$A_i = \frac{P_i}{\sum_{i=1}^{n} P_i} S. \tag{10}$$

6. Summary

Three different types of day-ahead natural gas consumption forecast

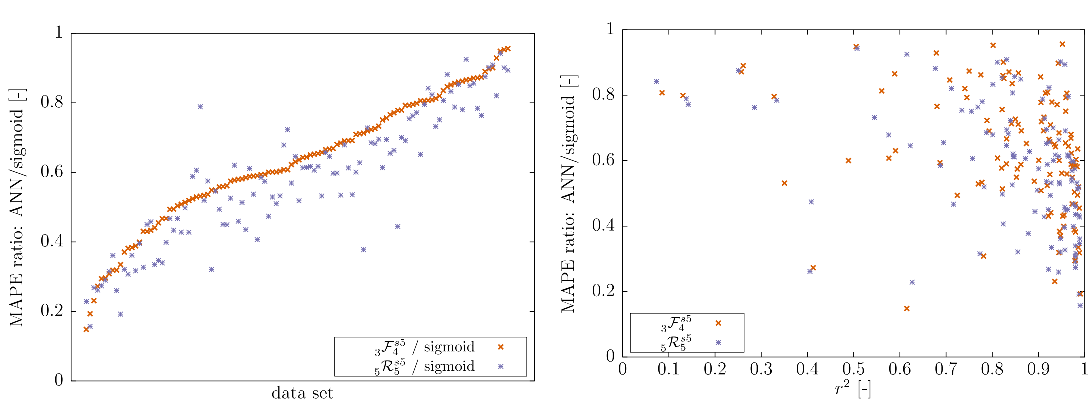

Fig. 10. The ratio of the neural network MAPE and sigmoid model MAPE for all data sets is shown in the left panel. Data sets were sorted to improve readability of the plot. In the right panel the correlation between MAPE ratio and square of the Pearson sample correlation coefficient is shown.

models have been developed in this paper: The sigmoid regression model, the feed-forward neural network model and the recurrent neural network model. The models were developed for 115 different gas metering stations, which were located in different climate zones (Mediterranean, Alps, Pannonia). The applicability of the developed models depends on the fact that the gas supply company must have access to the temperature forecast for the next day for the region where its consumers are located.

The sigmoid regression models are easy to develop, since only a nonlinear fitting algorithm has to be implemented to determine the model constants. From an implementation point of view, they are also easy to integrate into spreadsheet software and are, therefore, readily available to gas utilities. However, as we have shown in this paper, their accuracy is lower than the accuracy of models based on artificial neural networks. The computational resources required for neural network training are considerable, but they are not a limiting factor for use. In fact, a gas company would need to train its networks on an annual basis for perhaps a dozen of its characteristic consumers. Even if this technology were applied to entire countries, the number of neural networks to be trained would not exceed a thousand, resulting in annual computing times in the order of weeks. The use of trained neural networks in the daily operation of gas supply companies requires the development of special software, but the computing resources are small. Daily forecasts based on neural networks for thousands of consumers can be generated in a few minutes.

When modelling temperature-dependent gas consumers with neural network models we have shown a reduction of the forecast error by up to 5 times compared to the sigmoid regression model. For consumers whose gas consumption is not fully temperature-dependent, the error reduction is about 2 times. Based on these results, and since the computational requirements for neural network models are large but manageable, we conclude that the use of neural network-based models is preferable to sigmoid regression. Looking at MAPE, the ANNs are able to reach an error of 5%–10% in the entire temperature range for day-ahead forecasting of temperature-dependent gas consumers. The sigmoid model matches this accuracy only in the case of low outside temperature (below $5^\circ C$), while at temperatures above this threshold, the error increases to about 30%–40%. The users, which are only partially temperature-dependent (i.e. the gas is used for heating as well as for industrial processes), present a limitation for the use of neural network models. The reason being that the forecast accuracy is greatly reduced. We observe a reduction of the square of the Pearson sample correlation coefficient from 0.98 to 0.5 in such cases. Gas utility companies are advised to instal independent continuous measurement of industrial users of gas and model only temperature dependent users.

We investigated feed-forward and recurrent neural networks with different characteristics (number of size and hidden layers and activation function types). We found that the prediction accuracy of all versions of the artificial neural networks was of the same order of magnitude. For purely temperature-dependent data sets the square of the sample Pearson correlation coefficient was $r^2 > 0.98$. The best results were obtained with the recurrent neural network with a long input layer, considering the gas consumption in the last five days, the average gas day temperature in the last four days, and the predicted average temperature for the next gas day to estimate the gas consumption for the next day.

Declaration of competing interest

The authors declare that they have no known competing financial interests or personal relationships that could have appeared to influence the work reported in this paper.

Appendix

Table 1
Values of the *A*, *B*, *C* and *D* constants for the sigmoid model.

data set	A	B	C	D	data set	A	B	C	D
1	3.216	−41.94	4.265	0.342	31	3.372	−36.46	7.532	0.256
2	3.659	−42.58	3.93	0.255	32	2.874	−34.01	6.515	0.182
3	2.74	−37.19	5.464	0.297	33	1.551	−30.43	8.56	0.399
4	0.428	−16.77	4.281	0.66	34	3.383	−34.89	7.115	0.131
5	4.585	−45.35	4.437	0.263	35	−1.677	−2.17	0.403	2.227
6	2.965	−40.58	4.629	0.351	36	3.448	−34.43	4.925	−0.099
7	1.9	−30.67	7.865	0.477	37	2.064	−31.85	8.236	0.265
8	4.062	−40.35	4.231	−0.019	38	2.725	−31.14	8.317	0.004
9	0.045	−30.15	−1937.688	0.975	39	2.659	−37.04	6.685	0.28
10	121.76	−337.07	2.23	0.441	40	19.335	−63.69	4.875	−0.021
11	3.588	−40.35	4.528	0.228	41	2.414	−34.82	5.468	0.139
12	2.556	−31.49	6.982	0.308	42	3.511	−38.89	4.499	−0.148
13	3.653	−39.68	4.254	0.163	43	2.744	−34.39	5.138	−0.047
14	4.05	−41.67	4.46	0.192	44	3.089	−36.33	5.288	0.002
15	0.231	−24.28	48.011	0.882	45	2.327	−32.59	6.312	0.029
16	3.524	−41.02	4.644	0.257	46	3.148	−37.1	5.987	0.062
17	1.326	−31.05	8.581	0.7	47	4.588	−45.94	4.091	0.201
18	3.582	−38.15	5.055	0.17	48	0.424	−18.76	4.472	0.651
19	3.295	−33.19	8.134	0.023	49	3.064	−34.91	5.26	−0.118
20	3.179	−34.3	7.126	0.108	50	2.264	−34.82	6.244	0.196
21	2.451	−30.87	7.293	0.113	51	3.826	−41.11	5.078	0.167
22	3.042	−34.16	6.526	0.023	52	2.798	−36.23	6.102	0.144
23	2.816	−32.42	9.864	0.119	53	2.529	−35.92	5.377	0.064
24	4.327	−46.67	4.413	0.476	54	2.91	−33.98	5.068	−0.087
25	5.356	−41.98	4.455	0.059	55	2.315	−34.86	5.448	0.206
26	2.734	−32.68	6.188	−0.086	56	4.532	−44.65	4.047	0.099
27	2.992	−33.91	7.594	0.129	57	2.099	−32.12	5.628	0.129
28	3.114	−32.71	6.028	−0.017	58	3.016	−36.97	4.102	0.042
29	1.989	−30.89	5.66	0.231	59	2.709	−34.44	6.294	0.133
30	4.573	−39.1	7.28	0.239	60	3.205	−39.32	4.647	0.163

Table 2
Values of the *A*, *B*, *C* and *D* constants for the sigmoid model, continued. The median for each parameter is also shown.

data set	A	B	C	D	data set	A	B	C	D
61	3.019	−39.27	5.3	0.252	89	3.598	−39.01	5.493	0.035
62	2.445	−39.17	7.319	0.336	90	1.771	−32.55	6.547	0.245
63	4.002	−46.3	3.749	0.195	91	2.931	−35.77	5.319	0.035
64	2.188	−31.59	5.493	−0.081	92	4.114	−39.78	6.467	−0.054
65	2.542	−35.13	4.776	0.108	93	6.692	−49.9	4.492	−0.016
66	1.887	−29.51	6.739	0.045	94	4.534	−43.96	5.198	0.176
67	3.517	−40.05	4.356	0.084	95	2.877	−35.75	6.131	−0.009
68	0.078	−20.73	−46.298	0.993	96	2.152	−35.22	6.973	0.371
69	2.017	−45.81	4.564	0.657	97	2.705	−36.11	4.954	0.1
70	5.189	−40.47	6.909	−0.055	98	5.443	−43.53	7.279	0.103
71	0.069	−23.06	266.852	0.949	99	3.269	−38.06	6.521	0.046
72	2.146	−36.68	6.409	0.347	100	2.484	−40.15	7.647	0.434
73	3.198	−43.34	8.3	0.551	101	3.161	−40.83	7.129	0.309
74	2.61	−39.75	6.337	0.374	102	1.97	−33.85	5.596	−0.008
75	3.588	−39.92	4.616	0.046	103	2.481	−35.53	7.171	0.084
76	2.113	−32.43	4.519	0.153	104	2.583	−37.46	5.043	0.105
77	4.912	−40.52	5.366	−0.073	105	2.191	−36.97	12.617	0.299
78	2.387	−35.39	6.878	0.193	106	2.142	−35.93	5.4	0.205
79	2.775	−36.62	7.123	0.093	107	2.664	−36.18	6.962	0.064
80	3.442	−38.36	4.035	−0.194	108	2.773	−39.32	5.561	0.191
81	2.811	−34.97	5.353	0.018	109	0.489	−31.93	6.556	0.772
82	2.908	−36.1	5.446	0.072	110	3.632	−40.19	9.045	0.047
83	0.036	−23.81	4819.742	0.975	111	2.15	−36.78	5.488	0.265
84	2.352	−36.18	7.761	0.291	112	5.076	−47.46	3.165	−0.285
85	3.839	−42.48	4.613	0.172	113	2.997	−41.64	5.091	0.186
86	2.972	−37.03	7.154	0.048	114	90.686	−110.75	4.224	0.31
87	3.57	−38.24	8.803	0.136	115	3.301	−38.72	8.525	0.133
88	3.004	−35.87	7.25	0.005	median	2.91	−36.46	5.493	0.153

References

Aguilera, Roberto F., Ripple, Ronald D., 2011. Using size distribution analysis to forecast natural gas resources in Asia Pacific. Appl. Energy 88 (12), 4607–4620.

Akpinar, Mustafa, Fatih Adak, M., Yumusak, Nejat, 2016. Forecasting natural gas consumption with hybrid neural networks — artificial bee colony. In: 2016 2nd International Conference on Intelligent Energy and Power Systems. IEPS, pp. 1–6.

Akpinar, Mustafa, Fatih Adak, M., Yumusak, Nejat, 2017. Day-ahead natural gas demand forecasting using optimized ABC-based neural network with sliding window technique: the case study of regional basis in Turkey. Energies 10 (6).

Akpinar, Mustafa, Yumusak, Nejat, 2017. Naive forecasting of household natural gas consumption with sliding window approach. Turk. J. Electr. Eng. Comput. Sci. 25, 30–45.

Akpinar, Mustafa, Yumusak, Nejat, 2019. Daily basis mid-term demand forecast of city natural gas using univariate statistical techniques. Gazi Universitesi Muhendislik Mimarlık Fakultesi Dergisi 35, 725–742.

Azadeh, A., Asadzadeh, S.M., Mirseraji, G.H., Saberi, M., 2015. An emotional learning-neuro-fuzzy inference approach for optimum training and forecasting of gas consumption estimation models with cognitive data. Technol. Forecast. Soc. Change 91, 47–63.

Bai, Yun, Li, Chuan, 2016. Daily natural gas consumption forecasting based on a structure-calibrated support vector regression approach. Energy Build. 127, 571–579.

Bell, Jason, 2015. Machine Learning: Hands-On for Developers and Technical Professionals. John Wiley & Sons, Inc.

Beyca, Omer Faruk, Ervural, Beyzanur Cayir, Tatoglu, Ekrem, Ozuyar, Pinar Gokcin, Zaim, Selim, 2019. Using machine learning tools for forecasting natural gas consumption in the province of Istanbul. Energy Econ. 80, 937–949.

Chávez-Rodríguez, Mauro F., Dias, Luís, Simoes, Sofia, Seixas, Júlia, Adam, Hawkes, Alexandre, Szklo, Andre, F., Lucena, P., 2017. Modelling the natural gas dynamics in the Southern Cone of Latin America. Appl. Energy 201, 219–239.

Chen, Jie, Zeng, Guo Qiang, Zhou, Wuneng, Du, Wei, Lu, Kang Di, 2018. Wind speed forecasting using nonlinear-learning ensemble of deep learning time series prediction and extremal optimization. Energy Convers. Manag. 165 (March), 681–695.

Chen, Ying, Xu, Xiuqin, Koch, Thorsten, 2020. Day-ahead high-resolution forecasting of natural gas demand and supply in Germany with a hybrid model. Appl. Energy 262, 114486.

Erdogdu, Erkan, 2010. Natural gas demand in Turkey. Appl. Energy 87 (1), 211–219.

Farzaneh-Gord, Mahmood, Rahbari, Hamid Reza, 2018. Response of natural gas distribution pipeline networks to ambient temperature variation (unsteady simulation). J. Nat. Gas Sci. Eng. 52 (January), 94–105.

Forouzanfar, Mehdi, Doustmohammadi, Ali, Bagher Menhaj, M., Hasanzadeh, Samira, 2010. Modeling and estimation of the natural gas consumption for residential and commercial sectors in Iran. Appl. Energy 87 (1), 268–274.

Gascon, Alberto, Sanchez-Ubeda, Eugenio F., 2018. Automatic specification of piecewise linear additive models: application to forecasting natural gas demand. Stat. Comput. 28 (1), 201–217.

Hellwig, Mark, 2003. Entwicklung und Anwendung parametrisierter Standart-Lastprofile. PhD thesis. Technische Universität München.

Herbert, J.H., jan 1987. Analysis of monthly sales of natural gas to residential customers in the United States. Energy Syst. Pol. (United States) 10 (2).

Hribar, Rok, Potocnik, Primoz, Silc, Jurij, Gregor, Papa, 2019. A comparison of models for forecasting the residential natural gas demand of an urban area z Poto. Energy 167, 511–522.

Ivezić, Dejan, 2006. Short-term natural gas consumption forecast. FME Trans. 34, 165–169.

Karabiber, Orhan Altuğ, George, Xydis, 2020. Forecasting day-ahead natural gas demand in Denmark. J. Nat. Gas Sci. Eng. 76, 103193.

Karasalihović, Daria, Maurović, Lidia, Šunjerga, Snježana, 2003. Natural gas in Croatia's energy-future. Appl. Energy 75 (1–2), 9–22.

Laib, Oussama, Khadir, Mohamed Tarek, Mihaylova, Lyudmila, 2019. Toward efficient energy systems based on natural gas consumption prediction with LSTM Recurrent Neural Networks. Energy 177, 530–542.

Ma, Xin, Liu, Zhibin, 2017. Application of a novel time-delayed polynomial grey model to predict the natural gas consumption in China. J. Comput. Appl. Math. 324, 17–24.

Panapakidis, Ioannis P., Dagoumas, Athanasios S., 2017. Day-ahead natural gas demand forecasting based on the combination of wavelet transform and ANFIS/genetic algorithm/neural network model. Energy 118, 231–245.

Potočnik, P., Govekar, E., 2010. Practical results of forecasting for the natural gas market. In: Natural Gas. Intech, pp. 371–392.

Potočnik, Primož, Soldo, Božidar, Šimunović, Goran, Šarić, Tomislav, Jeromen, Andrej, Govekar, Edvard, 2014. Comparison of static and adaptive models for short-term residential natural gas forecasting in Croatia. Appl. Energy 129, 94–103.

Potočnik, Primož, Thaler, Marko, Govekar, Edvard, Grabec, Igor, Poredoš, Alojz, 2007. Forecasting risks of natural gas consumption in Slovenia. Energy Pol. 35 (8), 4271–4282.

Press, W.H., Teukolsky, S.A., Vetterling, W.T., Flannery, B.P., 1997. Numerical Recipes - the Art of Scientific Computing, second ed. Cambridge University Press.

Ravnik, J., Hriberšek, M., 2019. A method for natural gas forecasting and preliminary allocation based on unique standard natural gas consumption profiles. Energy 180, 149–162.

Sabo, Kristian, Scitovski, Rudolf, Vazler, Ivan, Zekić-Sušac, Marijana, 2011. Mathematical models of natural gas consumption. Energy Convers. Manag. 52 (3), 1721–1727.

Shaikh, Faheemullah, Ji, Qiang, 2016. Forecasting natural gas demand in China: logistic modelling analysis. Int. J. Electr. Power Energy Syst. 77, 25–32.

Shaikh, Faheemullah, Ji, Qiang, Shaikh, Pervez Hameed, Mirjat, Nayyar Hussain, Uqaili, Muhammad Aslam, 2017. Forecasting China's natural gas demand based on optimised nonlinear grey models. Energy 140, 941–951.

Siemek, Jakub, Nagy, Stanislaw, Rychlicki, Stanislaw, may 2003. Estimation of natural-gas consumption in Poland based on the logistic-curve interpretation. Appl. Energy 75 (1–2), 1–7.

Soldo, Božidar, 2012. Forecasting natural gas consumption. Appl. Energy 92, 26–37.

Soldo, Božidar, Potočnik, Primož, Šimunović, Goran, Šarić, Tomislav, Govekar, Edvard, 2014. Improving the residential natural gas consumption forecasting models by using solar radiation. Energy Build. 69, 498–506.

Szoplik, Jolanta, 2015. Forecasting of natural gas consumption with artificial neural networks. Energy 85, 208–220.

Taspinar, Fatih, Celebi, Numan, Tutkun, Nedim, 2013. Forecasting of daily natural gas consumption on regional basis in Turkey using various computational methods. Energy Build. 56, 23–31.

Vištica, Nikola, Banovac, Eraldo, Pavlović, Darko, 2015. Gas consumption forecasting: evidence from the Croatian gas market. Proc. Inst. Civil Eng. Energy 168 (1), 16–29.

Yu, Feng, Xu, Xiaozhong, 2014. A short-term load forecasting model of natural gas based on optimized genetic algorithm and improved BP neural network. Appl. Energy 134, 102–113.

Zeng, Bo, 2017. Forecasting the relation of supply and demand of natural gas in China during 2015-2020 using a novel grey model. J. Intell. Fuzzy Syst. 32 (1), 141–155.

Zeng, Bo, Li, Chuan, 2016. Forecasting the natural gas demand in China using a self-adapting intelligent grey model. Energy 112, 810–825.

Zhang, Wei, Yang, Jun, 2015. Forecasting natural gas consumption in China by Bayesian model averaging. Energy Rep. 1, 216–220.

Zhao, Hongying, Wu, Lifeng, 2020. Forecasting the non-renewable energy consumption by an adjacent accumulation grey model. J. Clean. Prod. 275, 124113.

Zhu, L., Li, M.S., Wu, Q.H., Jiang, L., 2015. Short-term natural gas demand prediction based on support vector regression with false neighbours filtered. Energy 80, 428–436.